DECLASSIFIED
CLASSIFICATION CHANGED TO:
BY AUTHORITY OF: TID-1111
BY: N. Johnstone 10/19/56

CENTRAL RESEARCH LIBRARY
DOCUMENT COLLECTION

ORNL-32

cy 5 A

MARTIN MARIETTA ENERGY SYSTEMS LIBRARIES
3 4456 0251095 9

Contract W-35-058 eng, 71

* * * * * * * * * * * *

Section VI

G. Young, Section Chief

****

SHIELDING EFFICIENCY OF AN OXYCHLORIDE-IRON CONCRETE -- COMPARISON WITH HANFORD SHIELD

E. P. Blizard, C. E. Clifford, J. Cassidy

May 21, 1948

Date Received: 5/24/48 Date Issued: 6/7/48
Date Received Figures: 6/7/48

CENTRAL RESEARCH LIBRARY
DOCUMENT COLLECTION
LIBRARY LOAN COPY
DO NOT TRANSFER TO ANOTHER PERSON
If you wish someone else to see this document, send in name with document and the library will arrange a loan.

SHIELDING EFFICIENCY OF AN OXYCHLORIDE-IRON CONCRETE -- COMPARISON WITH HANFORD SHIELD

E. P. Blizard, C. E. Clifford, J. Cassidy

ABSTRACT

Radiation attenuation tests were made on both a Hanford shield sample and an iron aggregate oxychloride cement, the physical properties of which are given a companion Technical Division Report (ORNL-17). The measurements consisted of the detection of neutrons throughout the shield by means of gold foils and the detection of γ radiation through increasing thicknesses of shield by means of a collimated G. M. tube with a fixed geometry. These samples were exposed to a pile flux of approximately 10^{10} n/cm^2/sec. and an accompanying γ flux which extrapolated to about 12,000 R/Hr at the inner face of the shield.

Various arrangements of thermal shields were tested with both samples in an effort to determine qualitatively the effect on the production and transmission of γ rays with a variation of the capture medium in the first or thermal portion of shield sample. The results indicate that the gammas are reduced in number when boron is used in the front portion of shield, with or without an iron thermal shield. The neutron attenuation in the outer portions of the shield is essentially unaffected by the nature of the thermal shield. The MO and Hanford samples displayed approximately equal overall neutron attenuation. Gamma intensities were less throughout the MO sample than at corresponding points in the Hanford sample.

[redacted]

MARTIN MARIETTA ENERGY SYSTEMS LIBRARIES
3 4456 0251095 9

INTRODUCTION

A magnesium oxychloride iron aggregate concrete has been developed by this laboratory, and is described in a companion report, ORNL-17. The present report describes the transmission measurements which compare the shielding efficiency of this concrete with that of a facsimile of the Hanford shield.

TESTING FACILITY

Figure 9 (drawing B-3279) shows the iron-lined hole through the west face of the X pile shield. The pile is on the right, and a typical arrangement of shield sample blocks is shown in the hole.

This hole is on the discharge face, so that bare metal is visible down the 2"x2" charging channels. This fast-flux is enhanced by the addition of one slug at the discharge end of each channel. The next nearest metal loading is 74" from the west, or near face of the graphite.

Thermal neutron flux at the inner end of the shielding samples has been measured with a silver wire to be 5×10^9 n/cm^2/sec. Gamma flux, from extrapolation of ionization chamber readings in an ordinary concrete sample, is found to be about 12000 R/hr.

DESCRIPTION OF SAMPLES

Concrete samples were cast into a set of three forms, each 16" long, having four sides of ½" steel plate. In the cast blocks the two faces parallel to the pile face were finished concrete (no iron plate).

[redacted]

[redacted]

The colemanite (16% B by wt.) layers were made by enclosing the powder between thin sheets of aluminum, the edges being closed on a wooden frame. The B_2O_3 and glass wool were similarly enclosed. Each boron containing layer was designed to decrease thermal flux by a factor of about 10^8.

The Hanford facsimile is shown in Figure No.10 . It was fabricated by the local shops of mild steel and tempered masonite.*

METHODS OF MEASUREMENT

Neutrons

Neutron flux was measured by activation of gold foils imbedded in the shield samples. Although these measure thermal and resonance (4.8 ev.) flux, it is assumed that this is proportional to the total flux in the region, which is reasonable in a highly absorbing medium. Care was taken in the case of the laminated Hanford sample, to measure at corresponding points in each iron-masonite cycle, so that the ratio between thermal and fast flux would remain approximately the same. It is obvious that a thermal flux reading in the masonite is not comparable to one in the iron.

Gold foils were inserted in the Hanford sample by means of removable strips of ¼" thick masonite. The foils were taped to the strips at 4" intervals, and positioned in the masonite ½" from the iron-masonite interfaces. Foil dimensions were: 2½" x 1 9/16"x.005".

The foils were inserted in the concrete blocks by means of two 1½" I.D. heavy iron pipes. These were cast into the material, one horizontal and 4" from the inner face, the other vertical and 4" from the outer face.

---

*For actual thicknesses as built see Appendix A.

Inside each pipe was placed a paraffin cylinder 1½" O.D. 1" I.D. The foils were wrapped at 4" intervals on a 1" diameter wooden spindle which was inserted inside the cylindrical paraffin liner. The foils were imbedded in hydrogenous material to increase thermal activation, but this effect is not great (about a factor of 2 to 3 in a 1% B sample).

Gamma rays

Gamma rays were measured by means of a Geiger Muller counter arranged as shown in figure 17. Successive readings were taken with increasing thickness of shield in place in the facility hole.

As the useful range of Geiger tubes is only about 1000, it was necessary to vary the pile power level to extend the readings over the required attenuation. With this technique, care was taken to observe and correct for the counts due to radioactivity induced at the higher power level which appears disporportionately large with very low levels. Thus it was attempted to make sufficient measurements to determine the equilibrium gamma flux through each thickness.

It should be noted that no attempt has been made to separate the attenuation of the shields for primary sources of gammas and neutrons. Our measurements include the two coupling effects, that is, (n,γ) capture processes, inelastic scattering, and (γ,n) processes, such as may occur with deuterium in the shield. One would of course expect the (n,γ) processes to be very important, and the (γ,n) contribution to be negligible.

RESULTS

Neutron attenuation (hard component)

1. Hanford shield

Neutron measurements on the Hanford facsimile, with 10½" iron

thermal shield, as built, reveal an effective neutron relaxation length of 4.7 cms. over the first three biological layers. Borst (CP-1202) reported 4.8 cms. for the same measurement. It will be noted (Figure 1, Table II), however, that at shield depths of greater than 32 inches, there is a considerable increase in effective relaxation length which can be attributed at least in part to a hardening of the neutron spectrum. The iron thermal shield transmits a large percentage of intermediate energy neutrons, which are slowed to thermal in the masonite and detected there. It is doubtful if the low relaxation length would have been observed in the first few biological layers if fast neutron detectors had been used.

At the greatest thicknesses it is to be expected that a part of the foil activation arises from neutrons which have been scattered into the shield sample from the surrounding X-shield concrete. This effect would be expected to be most important in a laminated shield, since in a transverse direction neutrons do not encounter a balanced shield. Tables I and II show flux measurements made along the axis of the sample compared to others at the same shield depth but displaced horizontally or vertically. From these it can be seen that the transverse leakage factor cannot be excessive, but a quantitative evaluation will be forthcoming in a later report.

Table III shows a few measurements made at a later date which essentially duplicate those of Tables I and II. These indicate an internal consistency of measurement better than 3%.

Table IV reports data taken on a Hanford biological shield with a 3" iron thermal shield instead of the 10½" thickness as was used in the

actual piles. The neutron attenuation for these two cases is compared in Figure 1, where it will be seen that at large thicknesses the two are about equivalent.

2. MO type shield

The neutron attenuation of the magnesium oxychloride-iron aggregate concrete (MO) is compared to the Hanford biological shield in Figure 1. It will be seen that between thicknesses of 15 and about 35 inches, the two behave alike. Beyond this distance the transverse leakage into the Hanford material becomes predominant. From 40 to 48 inches, the readings exhibit a neutron relaxation length characteristic of the surrounding X shield. Further out than this the readings are scarcely above background and, hence, not very meaningful.

It is to be expected that MO and Hanford biological shields would be approximately alike for fast neutrons since their hydrogen concentrations are nearly the same. A comparison of their major constituents in Mg.-moles per c.c. is as follows:

	Density	Fe	H	Mg	O	C	Cl	N
W-biol.	4.27	64.0	42.3	-	21.7	26.5	-	1.0
MO	5.80	85.3	38.3	12.7	30.4	-	2.96	-

SLOW NEUTRONS-THERMAL SHIELDS

An iron thermal shield was used as the innermost shield component in the Hanford piles to absorb most of the energy in the radiation. This could be water-cooled, and thus no temperature stability problems were encountered. The power absorbed by this shield has been measured and found

 [redacted]

quite low*, so that it appears possible to utilize a thermal shield whose primary purpose is not to absorb heat, but to assist in the radiation attenuation.

The large thermal flux incident on the inner shield face produces many hard gammas due to capture, which adds definitely to the effective gamma source. Because boron absorbs neutrons readily with little or no capture gammas, it could be utilized to advantage in the thermal shield. Accordingly two boron-containing layers were constructed, of such thickness as to decrease thermal neutron flux by a factor of 10^8 (about 1 gm/cm^2.)

As is to be expected, these layers did not exhibit any effect upon the neutron attenuation at large thicknesses of shield, but the thermal flux in the first foot of shield is considerably reduced, with an accompanying reduction in capture gammas. This is demonstrated in Figure 2 in which 2" of colemanite is compared to 7½" Fe as a thermal shield. At large distances the flux is higher in the case in which iron is used, but this merely demonstrates that MO is a better neutron shield than the pure iron which displaced it. Similar effects will be noted in Figure 1. The Hanford biological shield was tested with two different thicknesses of iron thermal shield, and again the laminated iron and masonite appears better than the pure iron. Thus the ordinate (Figure 1) at 20" corresponds in one case to flux through 10½" Fe, 4½" masonite, 3 3/4" Fe, and 1¼" masonite, which is to be compared to the other reading at 20" representing flux through 3" Fe, 4½" masonite, 3 3/4" Fe, 4½" masonite, 3 3/4" Fe, and ½" masonite.

Figures 3 and 4 show the results of adding a second layer of boron at a point farther back in the shield. Measurements show that the

---

*See ORNL-17, page 9.

amount of boron used was not justified in this position. Data was also taken with a second boron-containing layer behind the 7½" Fe thermal shield.

GAMMA RAY ATTENUATION

Capture gamma rays formed within the shield considerably distort the gamma ray attenuation data taken behind successive thicknesses of shield. For example, the gamma flux behind 7½" of iron will vary considerably depending on the disposition of neutrons which are diffusing through. If there is essentially nothing behind the iron, then just the captures in iron will be measured (of course, plus transmitted primary gammas from the pile). On the other hand if the iron is followed by a moderator and absorber such as masonite, this rate of capture will increase considerably.

There is, therefore, some question as to which measurements should be taken - measurements in the shield, at various points, or measurements behind various thicknesses of shield. The purpose of the experiment is to learn about flux behind the whole shield, so if the total thickness can be chosen, then measurements of components which affect this flux are the interesting ones. For this reason, it is perhaps best to read fluxes in the shield, rather than behind partial shields. Both measurements can be useful, however, if correctly interpreted. Because of the physical difficulties attendant upon flux measurements in the shield, readings were taken in this instance behind successive thicknesses. It is hoped that with a new technique of measuring shield samples at the outside of the test hole, it will be possible to introduce detectors into various shield sections.

Gamma attenuation of the Hanford shield is shown in Figure 5 and Table 1a. The curve is not drawn through the point at 10" (equivalent) since this flux does not represent the situation in the shield, but rather behind a partial shield, as discussed above. For the other points, farther removed from the source, it may be assumed that the neutron flux has more nearly approached equilibrium, that all gamma flux measurements are similarly perturbed, and, therefore, are proportional to the flux at corresponding points in the shield.

Figure 6 shows the gamma attenuation data in MO type shielding. It is assumed that equilibrium is more nearly reached in the measurements on MO with a 2" colemanite thermal shield, so this attenuation is drawn in from lowest points for the data on other thermal shield arrangements. Because the boron-containing thermal shields were not of maximum available density, the data has been plotted against thicknesses corrected to a density of 5.8 gms/cm^3.

It is seen that the best thermal shield, from gamma attenuation considerations, is the single layer of colemanite (or other boron vehicle) at the innermost layer. This indicates furthermore the relative importance of capture gamma rays in the shielding problem.

Figure 5 also compares the Hanford shield with the MO and its colemanite inner layer, again on a density corrected basis. It is seen that even on this basis the MO plus colemanite is superior to the Hanford laminated shield. The rate of attenuation is about the same throughout the body of the shield, as would be expected when density corrections are made, but the flux at corresponding points is lowered by about a factor of two by the colemanite.

(It should be noted that a similar material, designated M1, since it contains 1% boron by weight, shows even better gamma attenuation, due to the inhibiting of capture gammas throughout the shield. Engineering difficulties with this material, however, including low density, make it a less desirable shield than MO.)

Figure 7 compares gamma attenuations of MO plus colemanite and MO plus 7½" Fe thermal shield with that of the Hanford shield as installed, on a density "as is" basis. As is to be expected, the MO, being considerably more dense, exhibits better characteristics.

It should be noted that the Hanford shield sample shows a lower attenuation in these tests than was observed by Zinn in another test (CP-684). If both sets of data are plotted against thickness of iron, our tests show an average relaxation length of 4.7 cms. of Fe, while Zinn's data gives 4.5 cms. of Fe for the first 45 cms., and 4.2 cms. for the next 20 cms. of Fe.

The penetration of gamma rays through thick targets has been treated by Bethe*, Hirschfelder, Magee and Hull**, Hirschfelder and Adams***, Harvey Hall, Sr.****, and Eugene Greuling*****. The effects of multiple scatterings are such that the attenuation is not exponential, but an exact treatment has not been made, to the knowledge of the authors.

---

* H. A. Bethe, A-4251.

** Phys. Rev. Vol. 73, No. 8 (April 15, 1948), page 852.

*** Phys. Rev. Vol. 73, No. 8 (April 15, 1948), page 863

**** DR-1033 Transmission of Gamma Rays Through Thick Layers, by Harvey Hall (of Navy Dept., Bu. Aer.)

***** Mon P-172, Bernstein et al; appendix by Greuling.

Bethe and Greuling assume essentially no angular deviation per scattering process, plus an assumption about the variation of cross section with energy degradation.

Hirschfelder and his collaborators essentially assume that all photons are scattered at the most probable angle, and calculate the contributions of successive scatterings.

The present data for the iron in the Hanford shield is plotted in Figure 8 along with normalized results of Zinn, and theoretical calculations of Bethe, and Hirschfelder and Adams.

One would expect the MO aggregate to be comparable on an iron-density basis with Hanford shield, and this is approximately true. There is, however, a small correction to be applied beyond the density factor for attenuation by pebbles compared to solid material. This has been pointed out by N. M. Smith, Jr., who has made a theoretical estimate of the magnitude of this extra correction*.

---

* CNL-21, N. M. Smith, Jr., The Absorption and Scattering of Radiation in Random Aggregates of Pebbles, issued 3/9/48.

[redacted]

TABLE I

NEUTRON ATTENUATION
Hanford Shield Facsimile
($10\frac{1}{2}$" Thermal Shield)

Run 16 exposed 2/9 - 2/16/48

	Gold Foil Activities After 7 Day Exposure at 3800 K.W.						
Distance From Center Line of Sample (Horiz. & Vert.) ⟶	12"	Up or Left 8"	4"	0	-4"	Down or Right -8"	-12"
Thickness of Sample Inches							
* 10.75	3.40×10^7	4.37×10^7	4.93×10^7	5.13×10^7	5.03×10^7	4.34×10^7	3.43×10^7
14.75	1.28×10^7			1.50×10^7			1.15×10^7
* 19	6.32×10^5			4.81×10^5			8.38×10^5
23		1.44×10^5	1.16×10^5	1.18×10^5	1.28×10^5	1.79×10^5	
* 27.25	2.21×10^4	9.79×10^3	7.07×10^3	6.92×10^3	7.74×10^3	1.42×10^4	4.46×10^4
31.25		9.24×10^3	3.35×10^3	2.01×10^3	2.30×10^3	4.30×10^3	
* 35.50		2.22×10^3		292		1.08×10^3	
39.50		791		109		255	
* 43.75	301	97.8	46.0	36.0	37.8	51.4	138
47.75		121	33.8	11.8	50.7	41.2	
* 52	81.9	17.9	8.1	6.8	8.4	11.9	35.2
56	141	26.9	6.7	3.1	3.6	36.3	20.2

* Horizontal (alternate with vertical).

[redacted]

TABLE II

NEUTRON ATTENUATION
Hanford Shield Facsimile
($10\frac{1}{2}$" Iron Thermal Shield)

Run 16 exposed 2/9 - 2/16/48

	Activities Normalized to 1 Day Exposure, Same Counter, etc. x.336						
Distance From Center Line of Sample (Horiz. & Vert.)	12"	Up or Left 8"	4"	0	-4"	Down or Right -8"	-12"
Thickness of Sample Inches							
*10.75	1.14×10^7	1.47×10^7	1.66×10^7	1.72×10^7	1.69×10^7	1.46×10^7	1.15×10^7
14.75	4.30×10^6			5.04×10^6			3.86×10^6
*19	2.12×10^5			1.62×10^5			2.82×10^5
23		4.84×10^4	3.90×10^4	3.96×10^4	4.30×10^4	6.01×10^4	
*27.25	7.43×10^3	3.29×10^3	2.38×10^3	2.33×10^3	2.60×10^3	4.10×10^3	1.50×10^4
31.25		3.11×10^3	1.12×10^3	675	773	1.44×10^3	
*35.50		745		98.1		363	
39.50		266		36.6		85.7	
*43.75	101	329	15.5	12.1	12.7	17.3	46.2
47.75		41	11.4	4.0	17.0	13.8	
*52	27.5	6.0	2.7	2.3	2.8	4.0	11.8
56	47.2	9.0	2.3	1.0	1.2	12.2	6.8

* Horizontal (alternate with vertical).

TABLE III

NEUTRON ATTENUATION
Hanford Shield Facsimile
($10\frac{1}{2}$" Iron "thermal" Shield)

Run 21 exposed 2/10 - 2/11/48

Thickness of Sample Inches	Gold Foil Activities Along Center Line of Sample - 1 Day Exposure
10.75	2.33×10^7
14.75	6.61×10^6
19	2.19×10^5
23	4.99×10^4

[redacted]

TABLE IV

NEUTRON ATTENUATION
Hanford Shield Facsimile
(3" Iron Thermal Shield)

Run 17 exposed 2/16 - 2/23/48

	Gold Foil Activities After 7 Day Exposure at 3800 K.W.						
Distance From Center Line of Sample (Horiz. & Vert.)	12"	Up or Left 8"	4"	0	-4"	Down or Right -8"	-12"
Thickness of Sample Inches							
*3.25	2.28×10^8			3.13×10^8			2.07×10^8
7.25		7.52×10^7		8.25×10^7		6.14×10^7	
*11.50	5.19×10^6	4.94×10^6	5.22×10^6	5.31×10^6	5.11×10^6	4.90×10^6	5.90×10^6
15.50		1.99×10^6		1.70×10^6		1.52×10^6	
*19.75	2.06×10^5	1.44×10^5	1.33×10^5	1.32×10^5	1.35×10^5	1.59×10^5	2.73×10
23.75		8.32×10^4	5.06×10^4	4.25×10^4	4.20×10^4	4.84×10^4	
*28	8.69×10^3			4.36×10^3			1.36×10^4
32		5.49×10^3		1.48×10^3		2.01×10^3	
*36.25	710	326	232	232	274	475	1370
40.25		640	191	98.3		163	
*44.50	129	44.1	27.4	26.1	37.8	73.9	305
48.50	506	117	29.1	12.8	11.0	23.7	67.3

* Horizontal (alternate with vertical).

TABLE V

[redacted]

NEUTRON ATTENUATION
Hanford Shield Facsimile
(3" Thermal Shield)

Run 17 exposed 2/16 - 2/23/48

	Gold Foil Activities Normalized to 1 Day Exposure						
Distance From Center Line of Sample (Horiz. & Vert.)	12"	Up or Left 8"	4"	0	-4"	Down or Right -8"	-12"
Thickness of Sample Inches							
*3.25	7.66×10^7			1.05×10^8			6.96×10^7
7.25		2.53×10^7		2.77×10^7		2.06×10^7	
*11.50	1.74×10^6	1.66×10^6	1.75×10^6	1.78×10^6	1.72×10^6	1.65×10^6	1.98×10^6
15.50		6.69×10^5		5.71×10^5		5.11×10^5	
*19.75	6.92×10^4	4.84×10^4	4.47×10^4	4.44×10^4	4.54×10^4	5.34×10^4	9.17×10^4
23.75		2.80×10^4	1.70×10^4	1.43×10^4	1.41×10^4	1.63×10^4	
*28	2.92×10^3			1.46×10^3			4.57×10^3
32		1.84×10^3		497		675	
*36.25	239	110	78.0	78.0	92.1	160	460
40.25		215	64.2	33.0		56.4	
*44.50	43.3	14.8	92.1	8.8	12.7	24.8	102
48.50	170	39.3	9.8	4.3	3.7	8.0	22.6

* Horizontal (alternate with vertical).

[redacted]

TABLE VI

NEUTRON ATTENUATION
MO Type Shield
($7\frac{1}{2}$" Iron "Thermal" Shield)
Run 22 Exposed 2/11-2/12/48

	Gold Foil Activities After 1 Day Exposure at 3800 K.W.				
Distance From Center Line of Sample (Horiz. & Vert.)	12"	Up or Left 8"	0	Down or Right -8"	-12"
Thickness of Sample Inches					
*11.50			7.66×10^6		
19.50		1.84×10^5	2.06×10^5	2.25×10^5	
*27.50	1.25×10^4		5.78×10^3		1.39×10^4
35.50	3.42×10^3		1.98×10^2		8.15×10^2
*43.50	71.3		8.2		136
51.50	113		-		15.8
	Inserts				
22			5.16×10^4		
38			53.4		

* Horizontal (alternate with vertical).

[redacted]

TABLE VII

NEUTRON ATTENUATION
MO Type Shield
(2" Colemanite - (wet) Thermal Shield)
Run 23 exposed 2/12 - 2/13/48

	Gold Foil Activities After 1 Day Exposure at 3800 K.W.						
Distance From center Line of Sample (Horiz. & Vert.)	12"	Up or Left 8"	4"	0	-4"	Down or Right -8"	-12"
Thickness of Sample Inches							
*1				3.44×10^6			
6				5.32×10^6			
*14		7.04×10^5	4.90×10^5	3.37×10^5	2.73×10^5	2.52×10^5	
22	2.97×10^4			1.91×10^4			2.67×10^4
*30	7.89×10^3	3.19×10^3	1.46×10^3	941	759	816	1.31×10^3
38	127			32.3			181
*46	132	60.7	2.4	-	-	18.0	8.4
	Inserts						
16.50				1.11×10^5			
32.50				249			

* Horizontal (alternate with vertical).

[redacted]

TABLE VIII

NEUTRON ATTENUATION
MO Type Shield
($7\frac{1}{2}$" Iron and 1" B_2O_3 Thermal Shield)
Run 24 exposed 2/13 - 2/17/48

	Gold Foil Activities for 4 Day Exposure			Activities Corrected to 1 Day Exposure Factor .338		
Distance From Center Line of Sample (Horiz. & Vert.)	Up or Left 4"	0	Down or Right -4"	Up or Left 4"	0	Down or Right -4"
Thickness of Sample Inches						
*12.50		1.64×10^7			5.56×10^6	
20.50	$4.8[illegible] \times 10^5$	4.44×10^5	4.38×10^5	1.65×10^5	1.50×10^5	1.48×10^5
*28.50	1.27×10^4	1.19×10^4	1.17×10^4	4.29×10^3	4.02×10^3	3.96×10^3
36.50	804	474	458	272	160	155
*44.50	21.3	21.0	23.6	7.2	7.1	7.97
52.50	37.7	3.0	1.2	12.7	1.0	.4
	Inserts			Inserts		
23		1.12×10^5			3.78×10^4	
39		137			46.3	
-55		514			1.8	

* Horizontal (alternate with vertical).

[redacted]

TABLE IX

NEUTRON ATTENUATION
MO Type Shield
(1" B_2O_3, 7½" Iron, 2" colemanite Thermal Shield)
Run 25 Exposed 2/17 - 2/18/48

Gold Foil Activities After 1 Day Exposure at 3800 K.W.			
Distance From Center Line of Sample (Horiz. & Vert.)	Up or Left 4"	0	Down or Right -4"
Thickness of Sample Inches			
*14.50	8.78×10^5	8.57×10^5	7.89×10^5
22.50	2.92×10^4	2.52×10^4	2.39×10^4
*30.50	1.07×10^3	981	1.04×10^3
38.5	105	50.7	48.2
*46.50	-	1.0	-

* Horizontal (alternate with vertical).

[redacted]

TABLE X

NEUTRON ATTENUATION
MO Type Shield
(2" Colmanite Thermal Shield and
2" Colmanite Behind First 16" MO)
Run 27 Exposed 2/19 - 2/20/48

Gold Foil Activities After 1 Day Exposure at 3800 K.W.			
Distance From Center Line of Sample (Horiz. & Vert.)	Up or Left 4"	0	Down or Right -4"
Thickness of Sample Inches			
*6		7.98×10^6	
14	4.89×10^5	4.55×10^5	4.32×10^5
*28	8.61×10^3	8.21×10^3	8.55×10^3
36	367	441	723
*44	26.1	25.1	29.0
52	12.5	7.2	7.3

* Horizontal (alternate with vertical).

TABLE (1a)

γ ATTENUATION
Run 28
Hanford Shield Facsimile
(10½" Thermal Shield)

Actual Thickness of Shield (Inches)	Thickness Corrected to Density of 5.8	Counts/min/kw on G M Tube	
		Total	Corrected Pile Background
7.5	10.16	266	266
24.38	22.73	5.17	5.16
34.5	31.22	.223	.213
49.5	40.97	.0177	.0075
61.38	52.02	.0102	.0007

TABLE (2a)

γ ATTENUATION
Run 23
MO Type Shield with
2" Calmanite Thermal Shield

Actual Thickness of Shield (Inches)	Thickness Corrected To Density of 5.8	Counts/min/kw on G M Tube	
		Total	Corrected Pile Background
18	16.7	18.0	17.9
34	32.7	.0843	.0725
50	48.7	.0118	.0007

[redacted]

TABLE (3a)

γ ATTENUATION
Run 22
MO Type Shield with
7.5" Fe Thermal Shield

Actual Thickness of Shield (Inches)	Thickness Corrected to Density of 5.8	Counts/min/kw on G M Tube	
			Corrected Pile Background
7.5	10.16	282	282
23.5	26.16	3.29	3.27
39.5	42.16	.0379	.0236
55.5	58.16	.0143	.000?

TABLE (4a)

γ ATTENUATION
Run 24
MO Type Shield with
7.75" Fe and 1" B_2O_3 Thermal Shield

Actual Thickness of Shield (Inches)	Thickness Corrected to Density of 5.8	Counts/min/kw on G M Tube	
		Total	Corrected Pile Background
8.75	10.5	133	133
24.75	26.5	1.88	1.87
40.75	42.5	.0277	.0192
56.75	58.85	.0085	.000

TABLE (5a)

γ ATTENUATION
Run 25
MO Type Shield with
7.5" Fe Thermal Shield Surrounded by Boron

Actual Thickness of Shield (Inches)	Thickness Corrected to Density of 5.8	Counts/min/kw on G M Tube	
		Total	Corrected Pile Background
8.75	10.5	117.3	117.3
10.75	11.2	90.3	90.3
26.75	27.2	.687	.66
42.75	43.2	.024	.0072
58.75	59.2	.0168	.000

TABLE (6a)

γ ATTENUATION
Run 27
MO Type Shield with
2" Colmanite Thermal Shield and
2" Colmanite Behind First 16" Block

Actual Thickness of Shield (Inches)	Thickness Corrected to Density of 5.8	Counts/min/kw on G M Tube	
		Total	Corrected Pile Background
18	16.7	17.6	17.6
20	17.4	13.4	13.4
36	33.4	.084	.073
52	49.38	.0107	.000

[redacted]

APPENDIX A

Hanford Shield Facsimile Dimensions
(thickness of layers only)

	Designed	Built
Block I:	7½" Fe	7½" Fe
Block II:	3" Fe	3 1/16" Fe
	4½" masonite	4 19/32 M
	3 3/4" Fe	3 13/16" Fe
	4½" masonite	4 5/8" M
	3/4" Fe	25/32" Fe
Block III:	3" Fe	3" Fe
(1st	4½" M	4 11/16" M
section)	2½" Fe	2½" Fe
(2nd	1¼" Fe	1 3/8" Fe
section)	4½" M	4 11/16" M
	3 3/4" Fe	3 13/16" Fe
	4½" M	4 11/16" M
	½" Fe	15/32" Fe
Block IV:	3¼" Fe	3 9/32" Fe
	4½" M	4 5/8" M
	3 3/4" Fe	3 3/4" Fe

Drawing # 5696

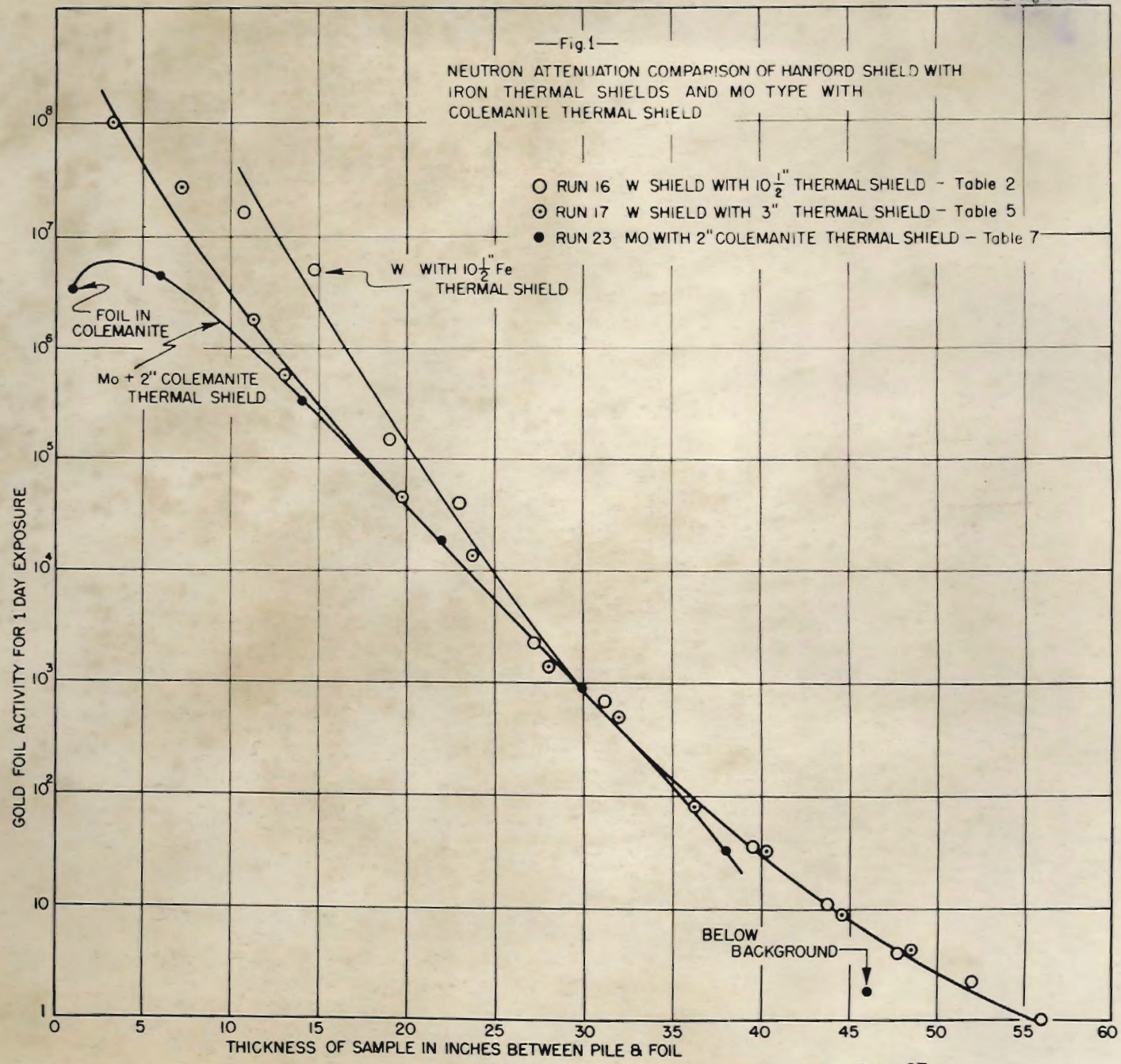

Drawing # 5697

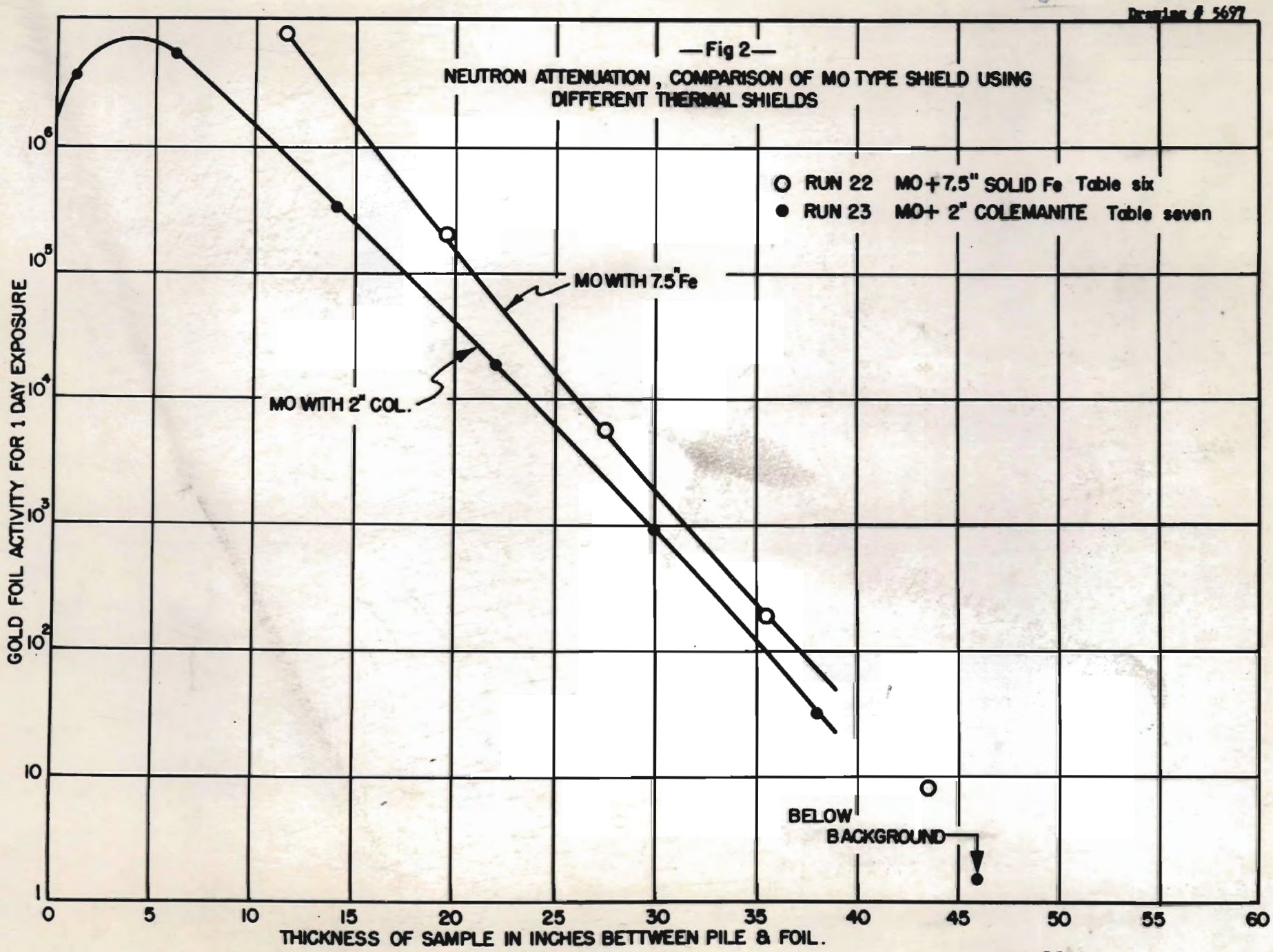

SECRET

Drawing # 5698

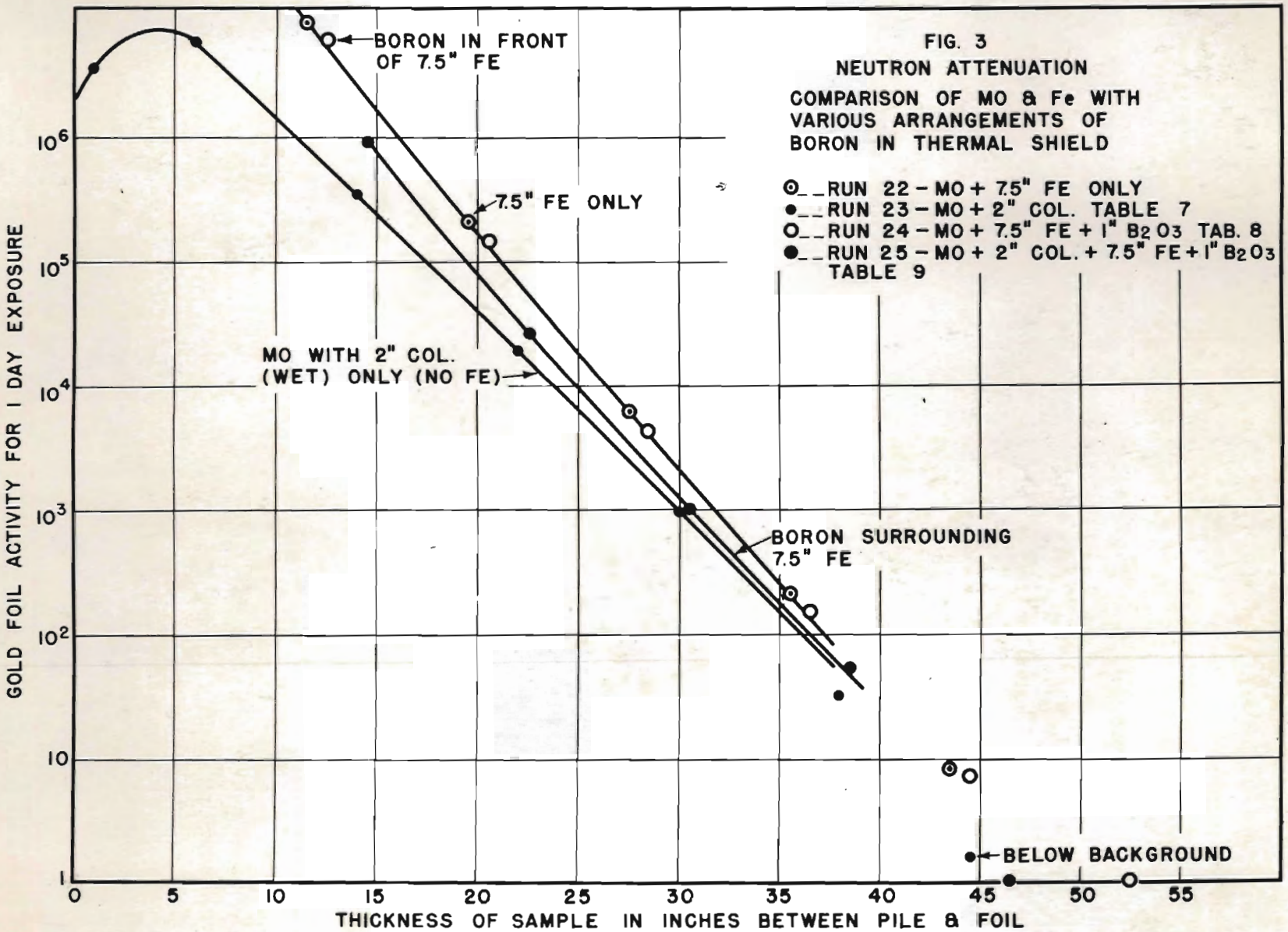

FIG. 3
NEUTRON ATTENUATION
COMPARISON OF MO & Fe WITH VARIOUS ARRANGEMENTS OF BORON IN THERMAL SHIELD

⊙ _ RUN 22 – MO + 7.5" FE ONLY
● _ RUN 23 – MO + 2" COL. TABLE 7
○ _ RUN 24 – MO + 7.5" FE + 1" B_2O_3 TAB. 8
● _ RUN 25 – MO + 2" COL. + 7.5" FE + 1" B_2O_3 TABLE 9

SECRET

Drawing # 5699

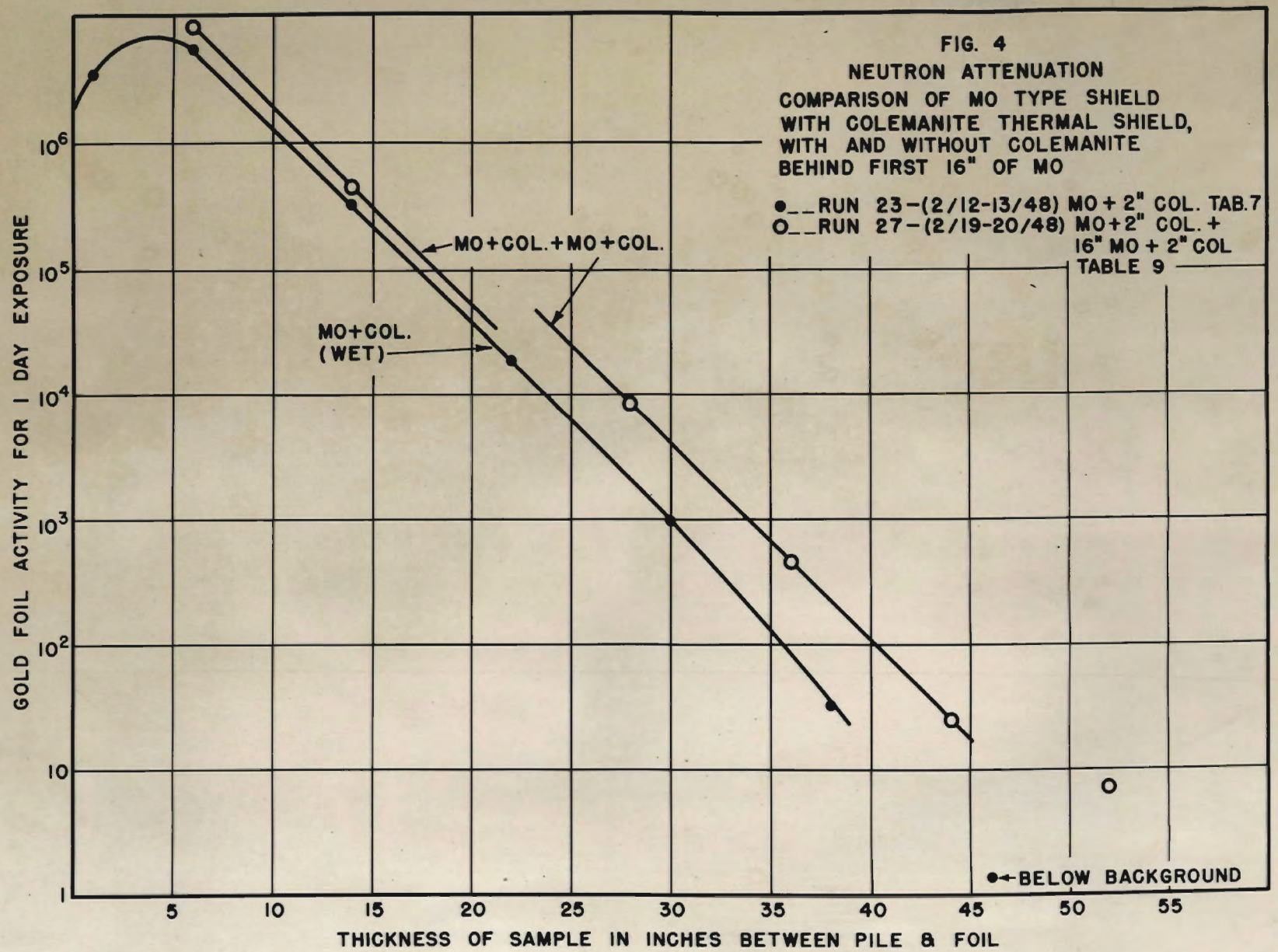

Drawing # 5700

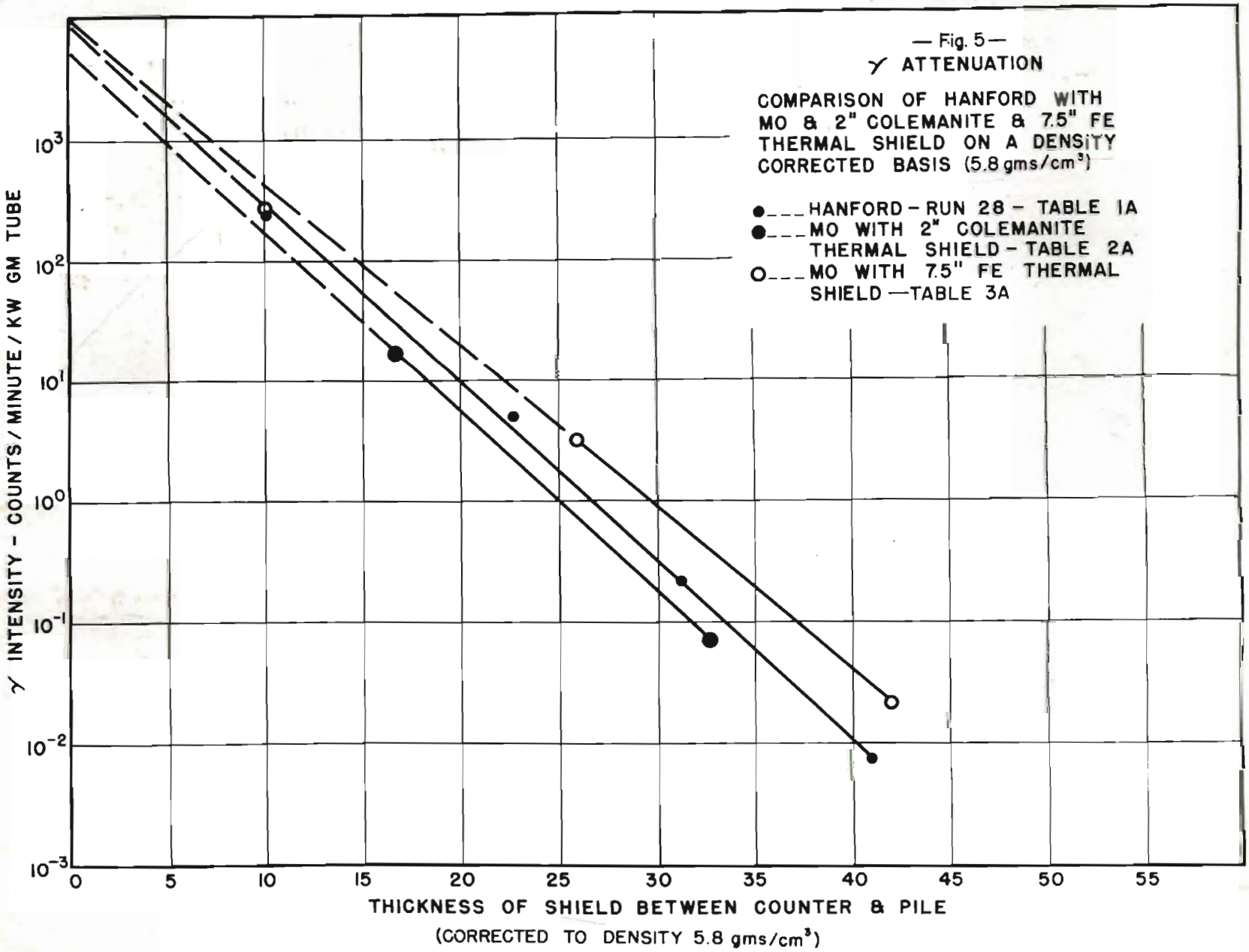

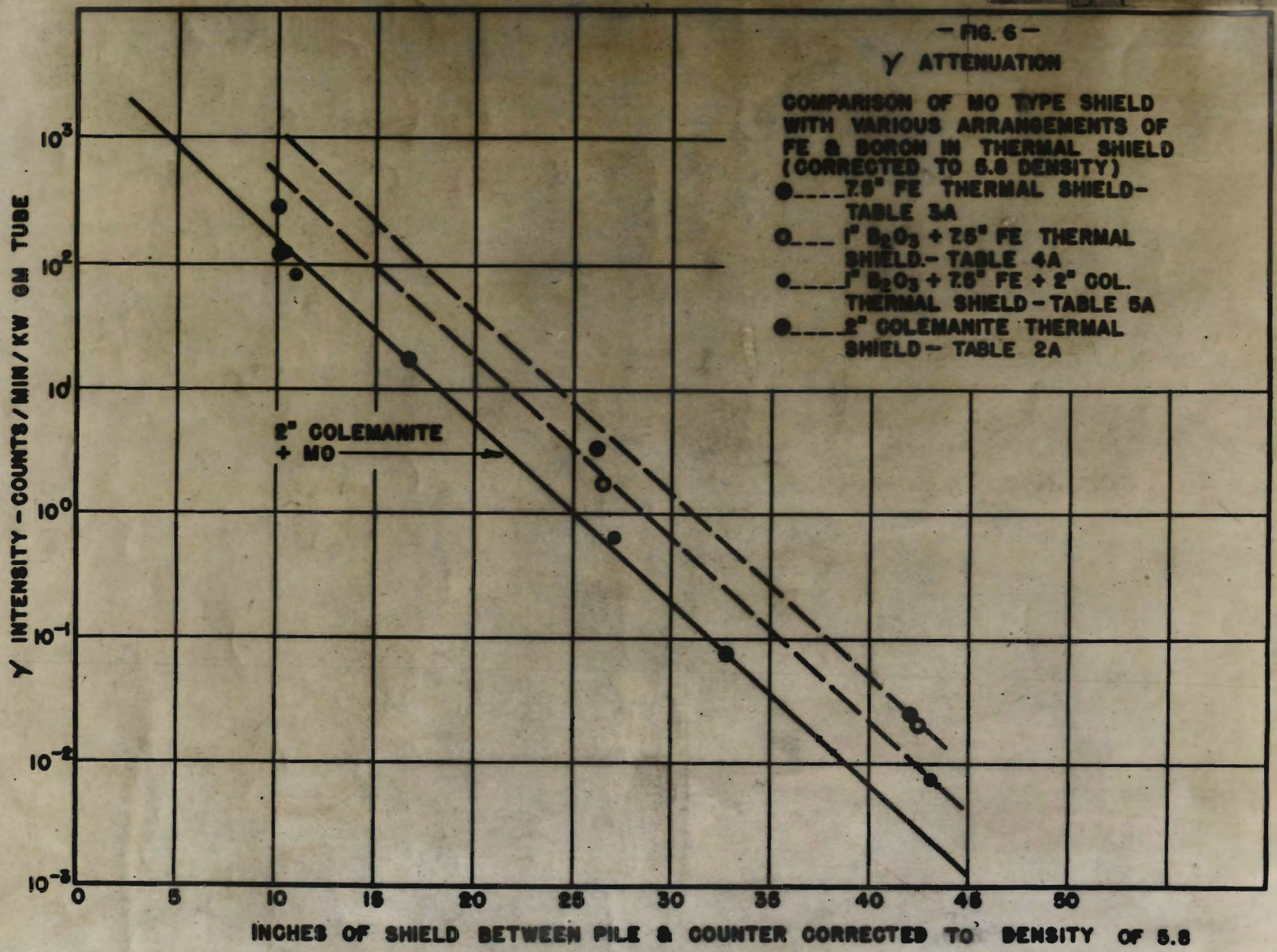
— FIG. 6 —
γ ATTENUATION
COMPARISON OF MO TYPE SHIELD WITH VARIOUS ARRANGEMENTS OF FE & BORON IN THERMAL SHIELD (CORRECTED TO 5.8 DENSITY)
●____7.5" FE THERMAL SHIELD- TABLE 3A
○___ 1" B_2O_3 + 7.5" FE THERMAL SHIELD.- TABLE 4A
●____1" B_2O_3 + 7.5" FE + 2" COL. THERMAL SHIELD - TABLE 5A
●____2" COLEMANITE THERMAL SHIELD - TABLE 2A
2" COLEMANITE + MO
γ INTENSITY - COUNTS / MIN / KW GM TUBE
10^3
10^2
10^1
10^0
10^{-1}
10^{-2}
10^{-3}
0
5
10
15
20
25
30
35
40
45
50
INCHES OF SHIELD BETWEEN PILE & COUNTER CORRECTED TO DENSITY OF 5.8

Drawing # 5702

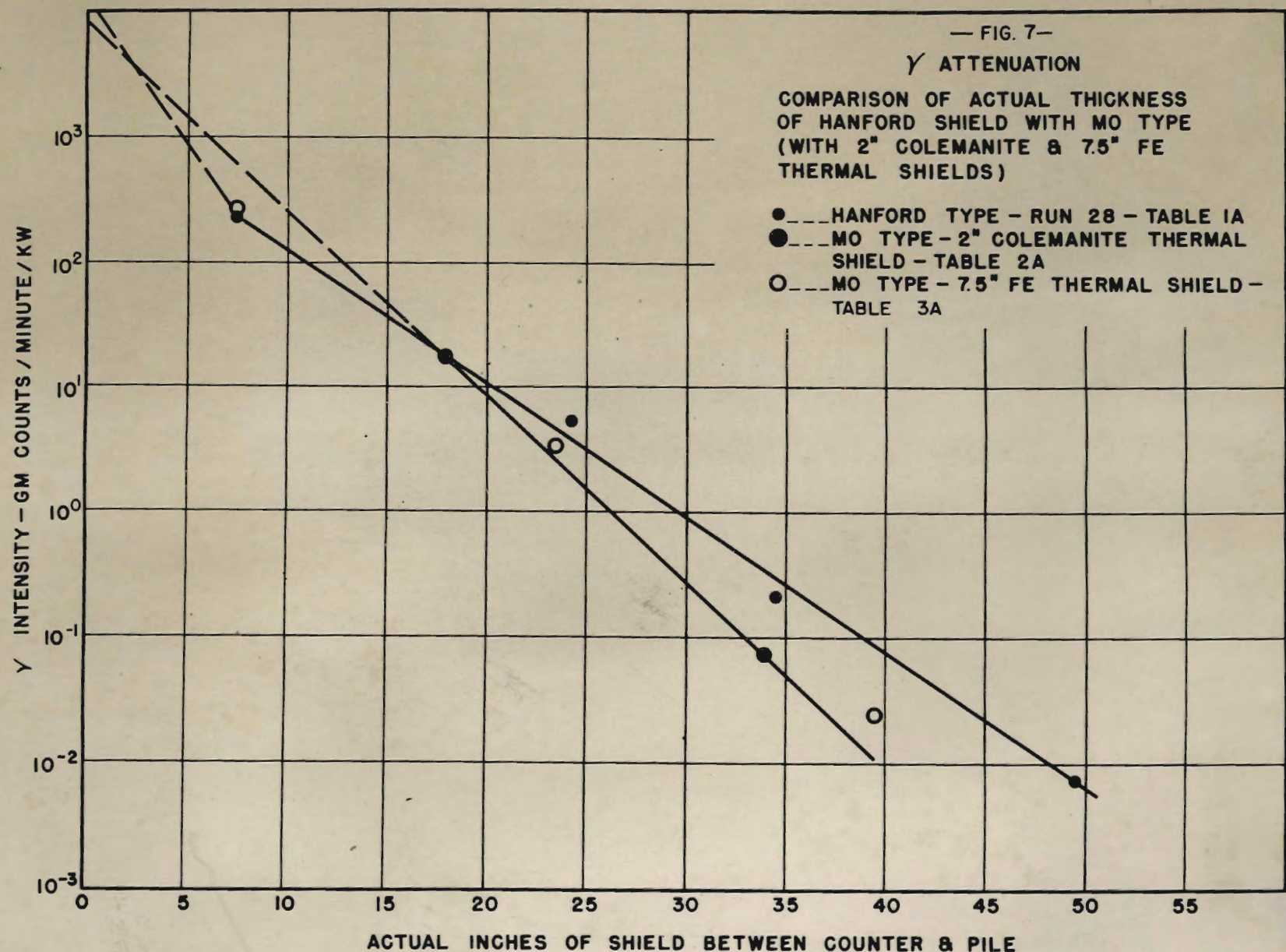

Drawing # 5703

—FIG. 8—

SECRET

γ- ATTENUATION

HANFORD MEASUREMENTS COMPARED TO THEORY AND OTHER MEASUREMENTS.

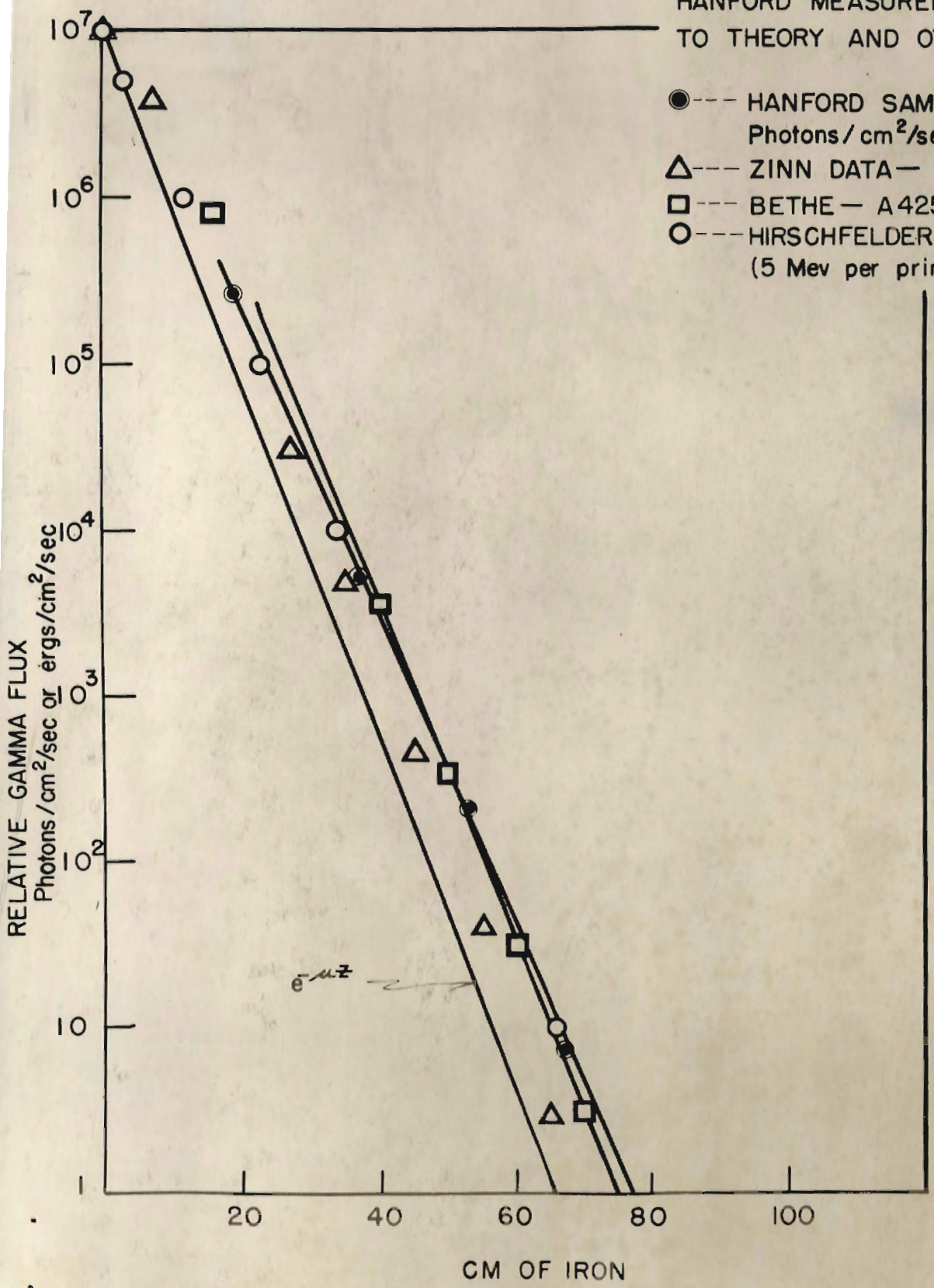

Confidential

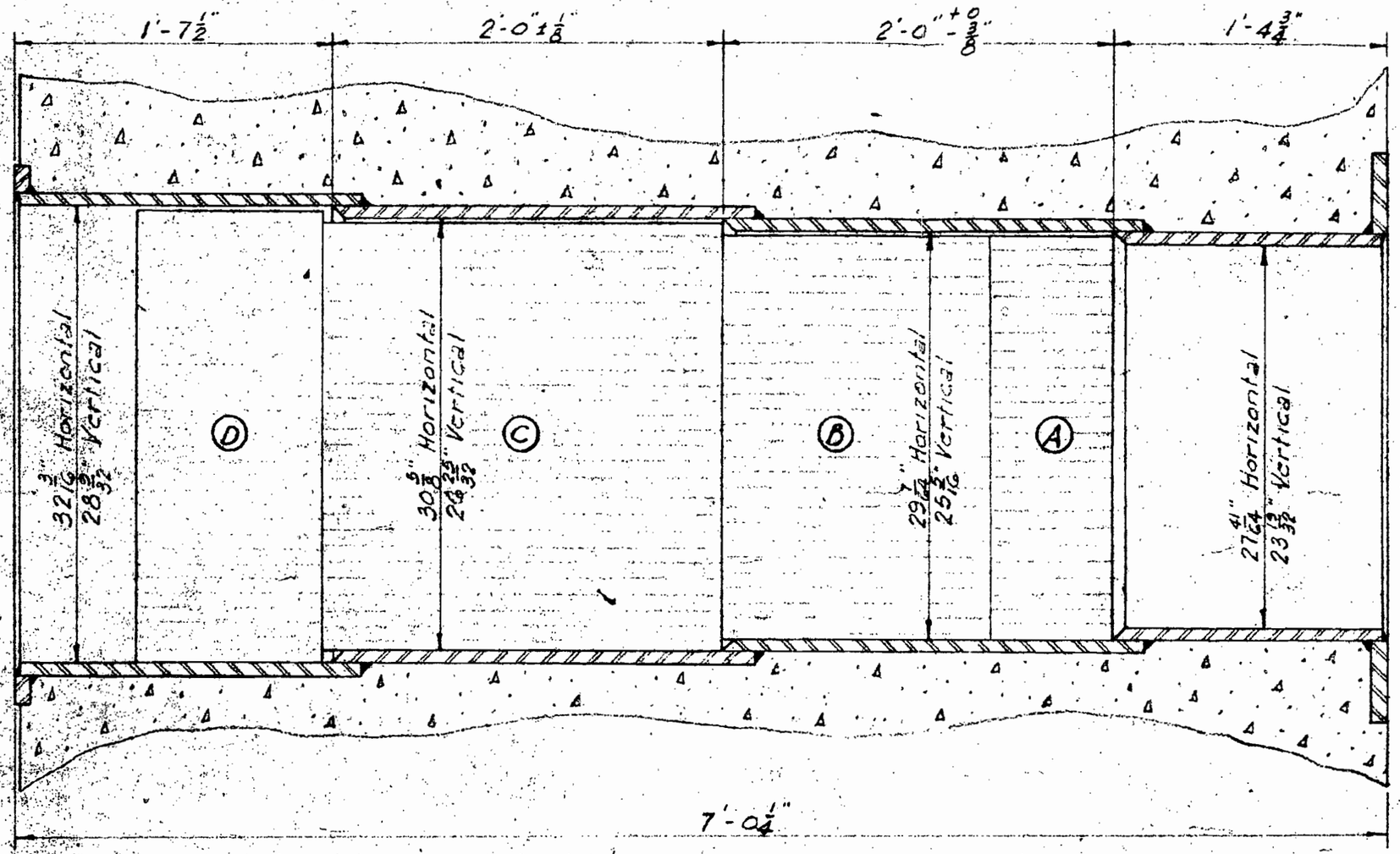

LAYOUT OF SHIELDING BLOCKS IN REAR CORE HOLE
ELEVATION SHOWN

This Drawing Classified As
Confidential
For

"This document contains restricted data within the meaning of the Atomic Energy Act of 1946 and/or information affecting the National defense of the United States within the meaning of the Espionage Act, 50 U.S.C. 31 and 32 as amended. Its transmission or the revelation of its contents in any manner to an unauthorized person is prohibited and may result in severe criminal penalty."

Confidential

REFERENCE DRAWINGS	DWG. Nº
EXPLODED ASSEM. OF BLKS.	C-3284
DETAILS OF REAR CORE HOLE	D-3166

REV. Nº	REVISION	APPROVED BY DATE
1	Added dimensions	JAH 11-21-47
1	Removed section of liner inside concrete.	JAH 11-21-47

BLDG. 105
LAYOUT OF SHIELDING BLOCKS IN REAR CORE HOLE

MONSANTO CHEMICAL COMPANY
CLINTON LABORATORIES
KNOXVILLE, TENN.

D. 10-31-47	C. H.G.D. 10/31/47	A. KLP 10/31/47	E. P.B. 10/31	
C.H.O.				
PROJ: C-316-R				
SCALE: 1/2" = 1'-0				B-3279

Confidential

A copy of this drawing can be obtained
In Lab Records at Oak Ridge National Laboratory

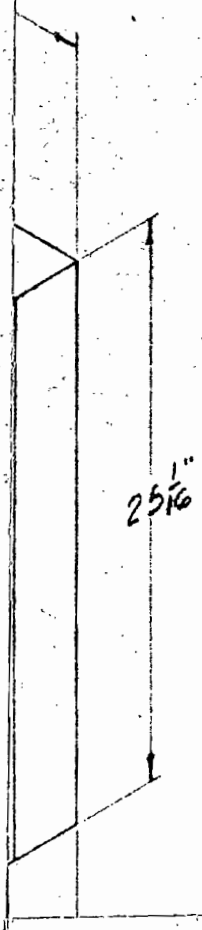

DETAIL OF FOIL HOLDERS						B-3285
BLDG. 105 EXPLODED ASSEMBLY OF SHIELDING BLOCKS						
MONSANTO CHEMICAL COMPANY CLINTON LABORATORIES KNOXVILLE, TENN.						
D. 10-31-47 C.H.O	C. H.G.D. 10/31/47	A. RSP 10/31/47	E. P.B. 10/31			
PROJ. C-316-R				C-3284		
SCALE: NONE						

SECRET

Drawing # 5704

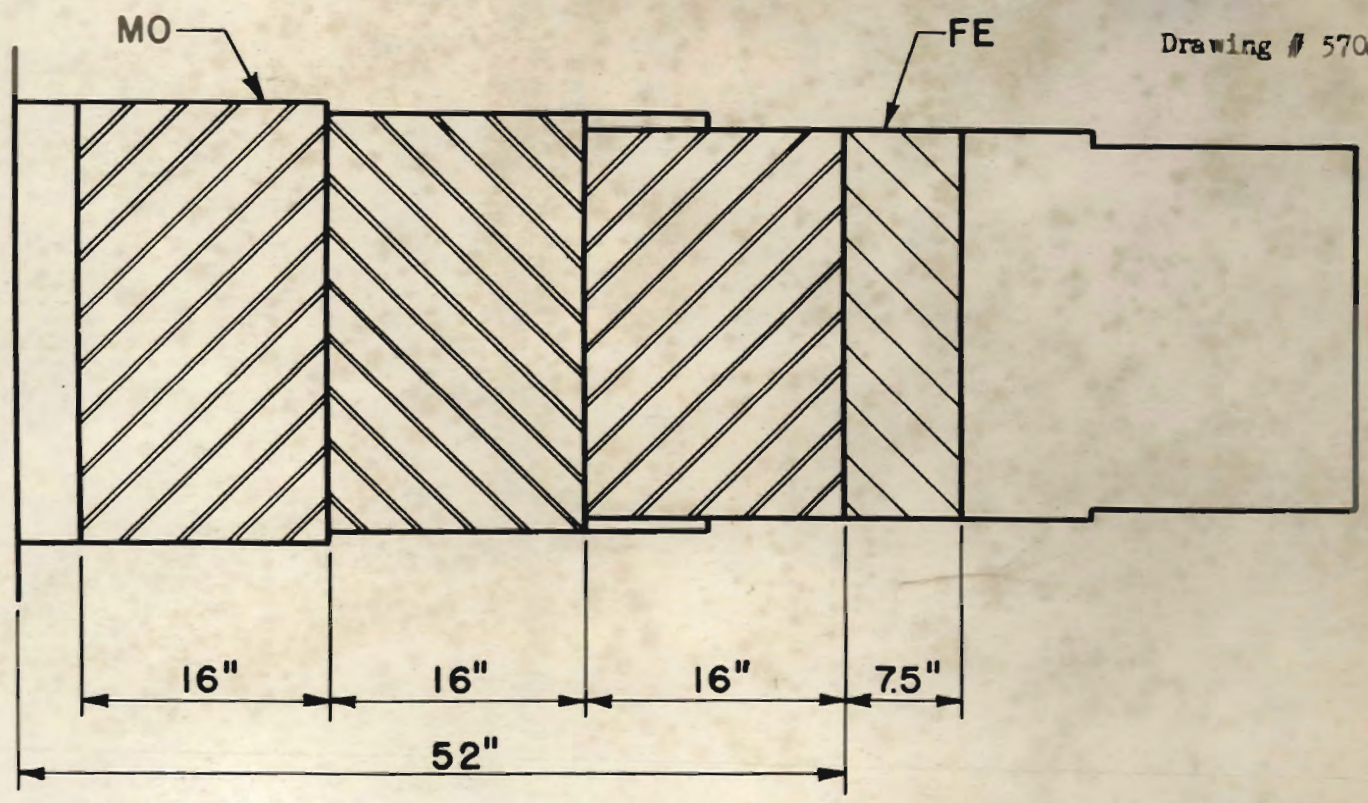

ARRANGEMENT FOR RUN 22

FIG. 11

SECRET

Drawing # 5705

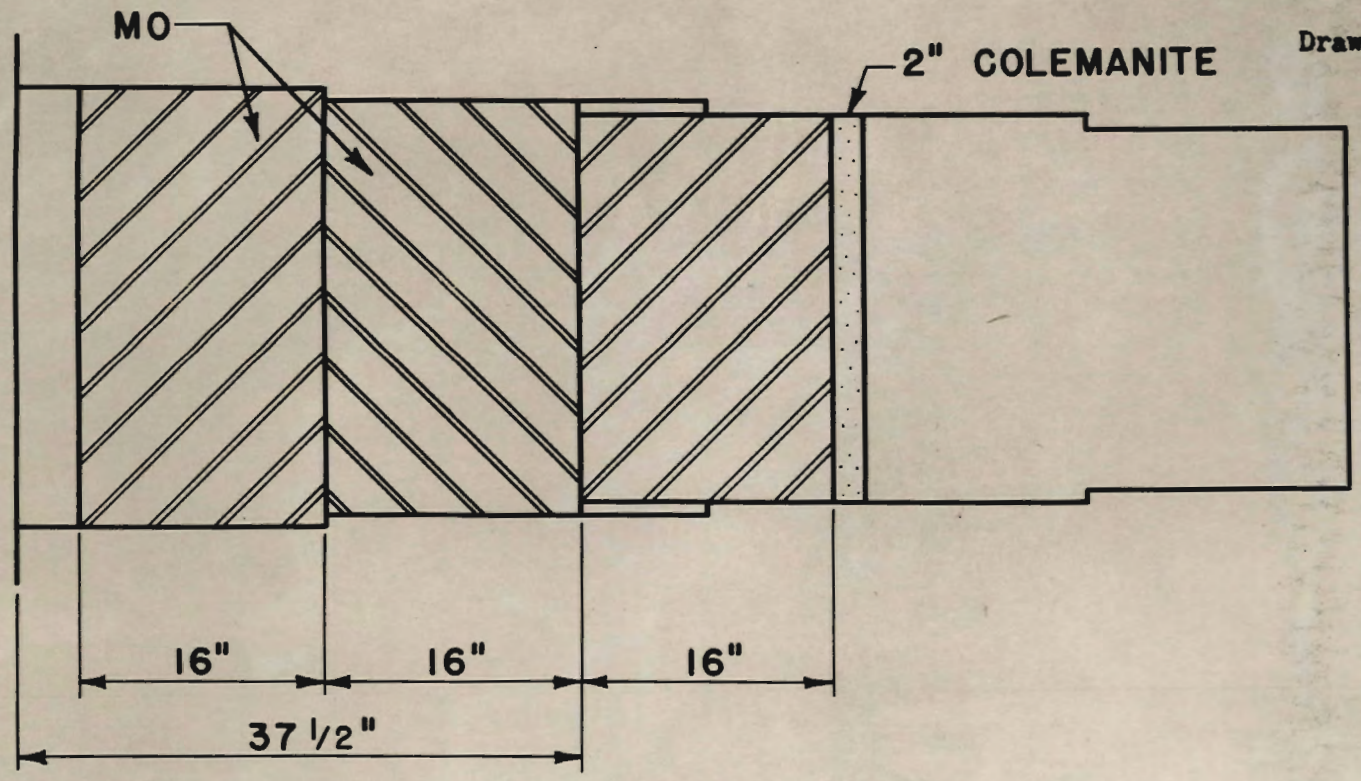

ARRANGEMENT FOR RUN 23

FIG. 12

SECRET

Drawing # 5706

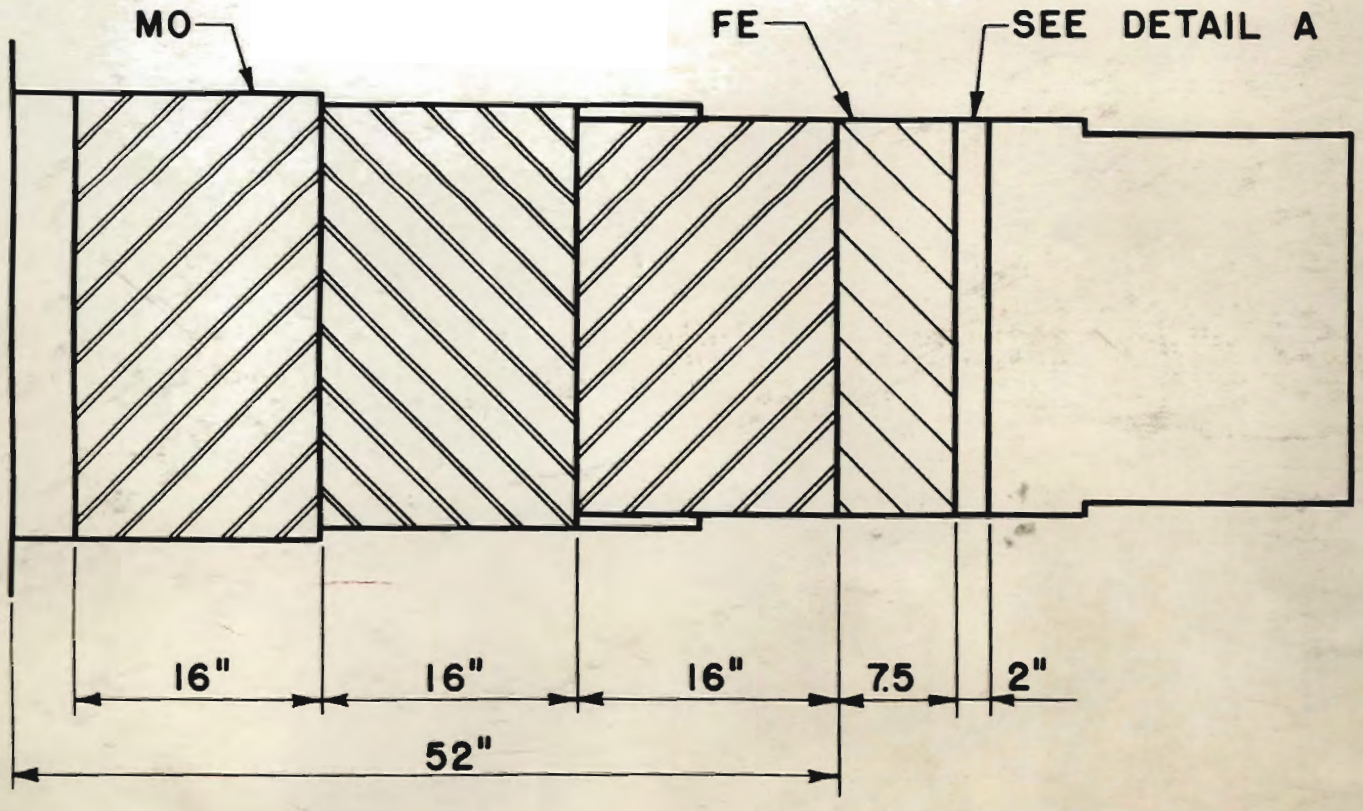

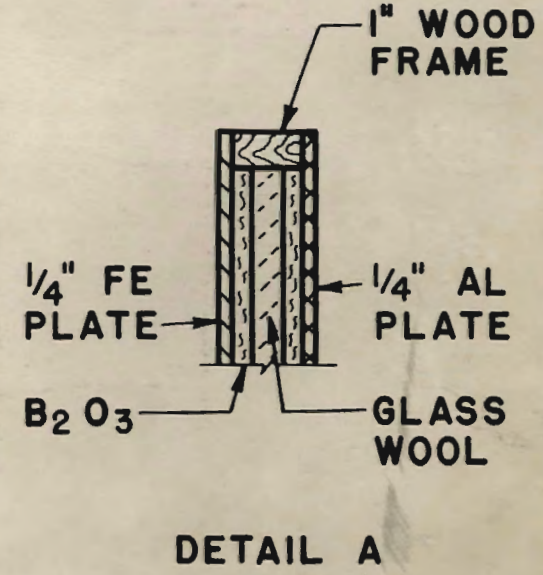

ARRANGEMENT FOR RUN 24
FIG. 13

SECRET

Drawing # 5707

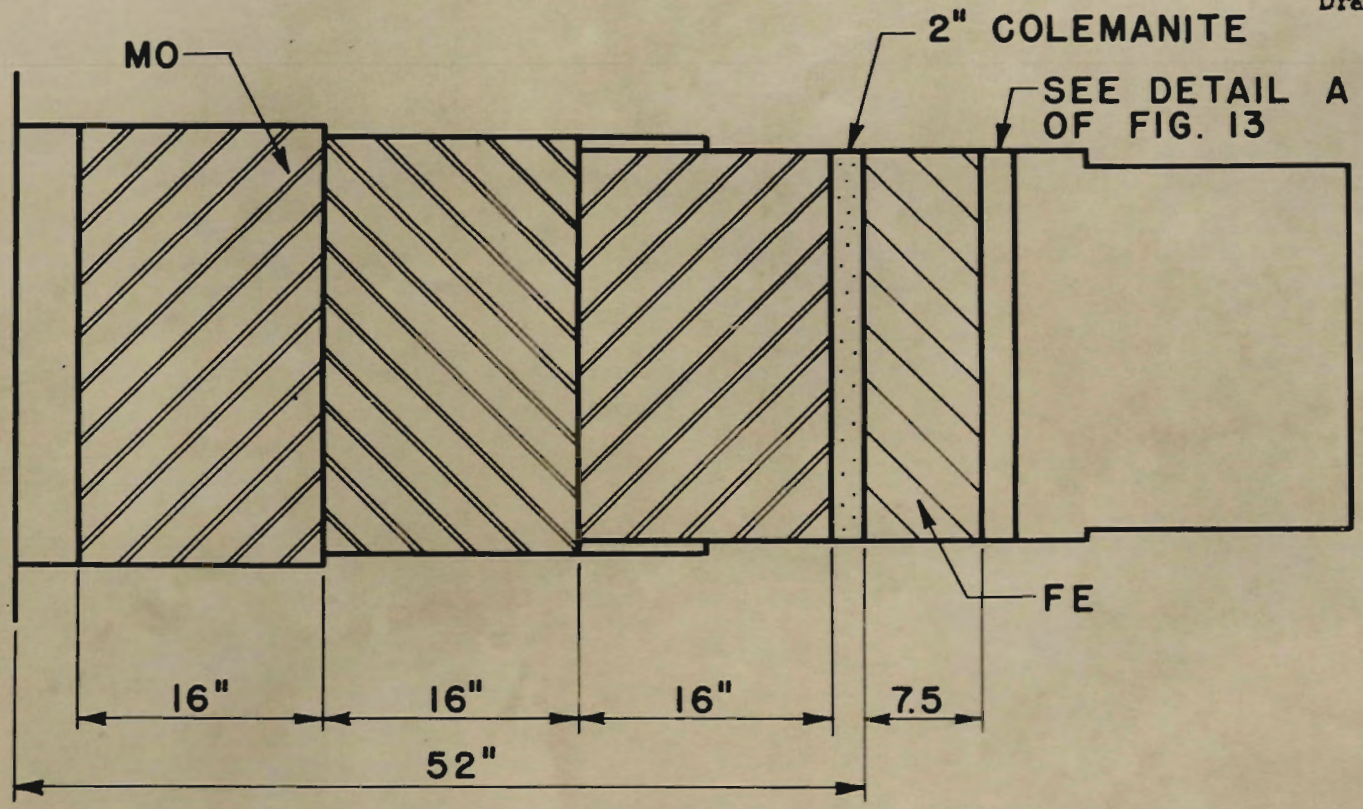

ARRANGEMENT FOR RUN 25
FIG. 14
PAGE 40

Drawing # 5708 SECRET

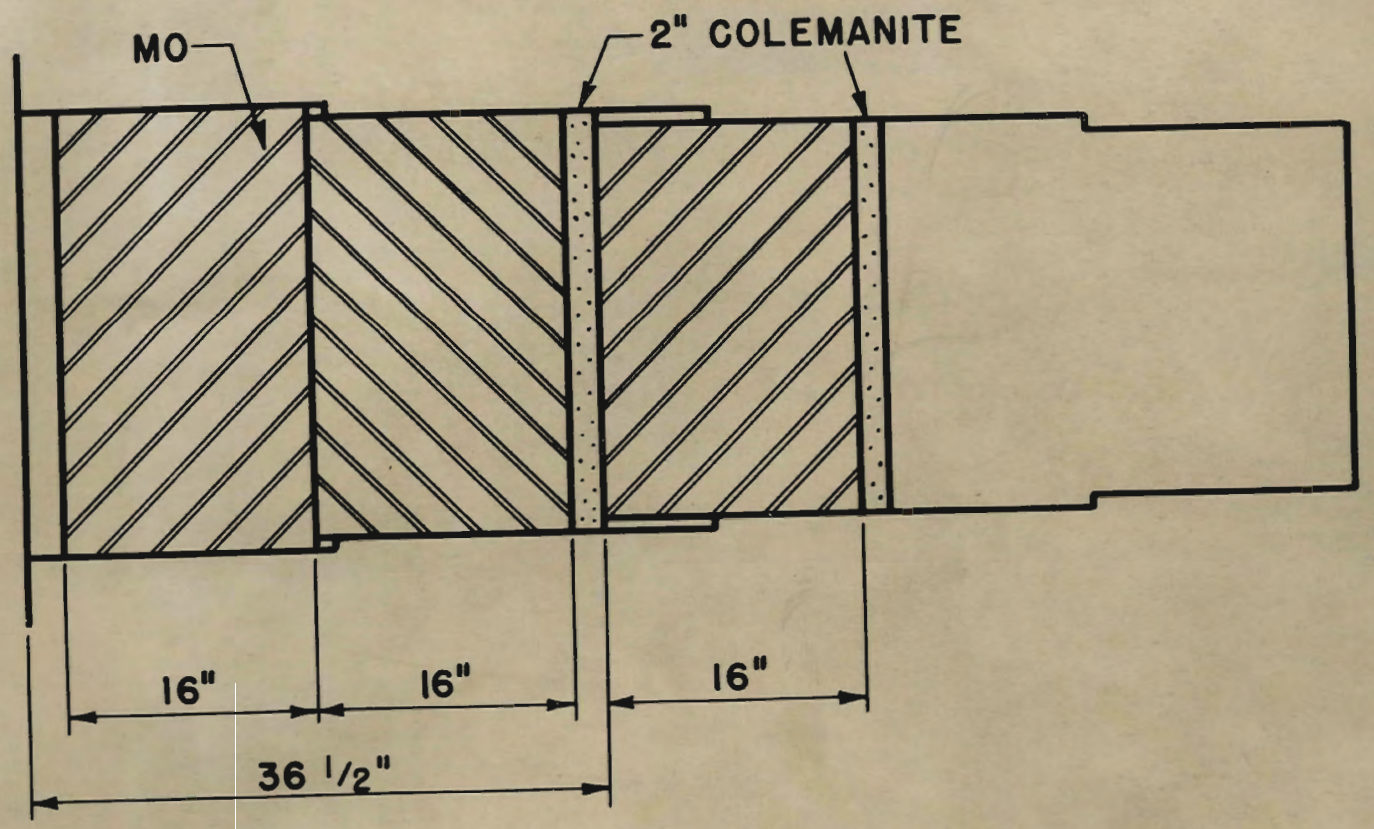

ARRANGEMENT FOR RUN 27
FIG. 15
PAGE 41

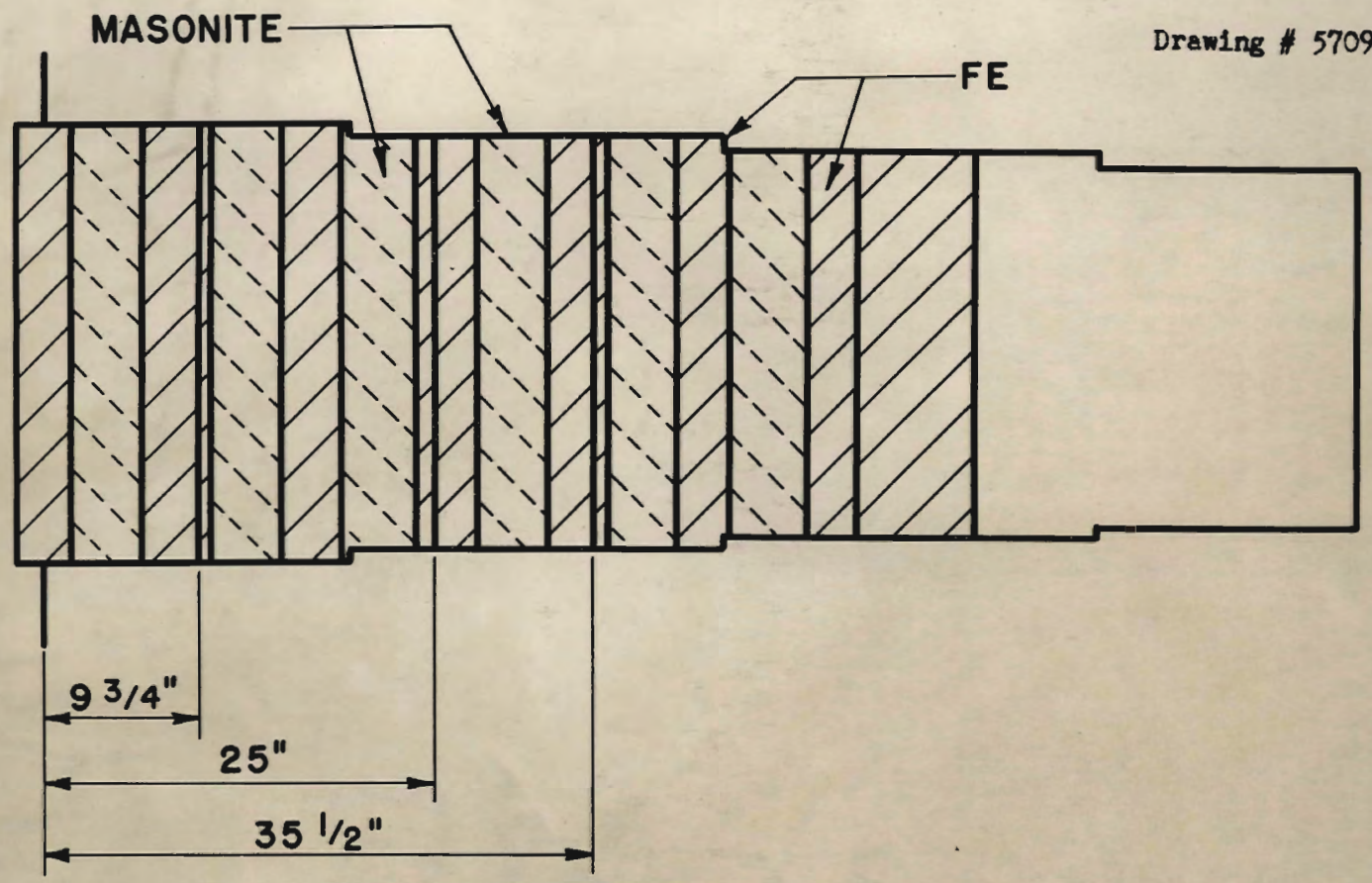

Drawing # 5709

SECRET

ARRANGEMENT FOR RUN 28

FIG. 16

SECRET

Drawing # 5710

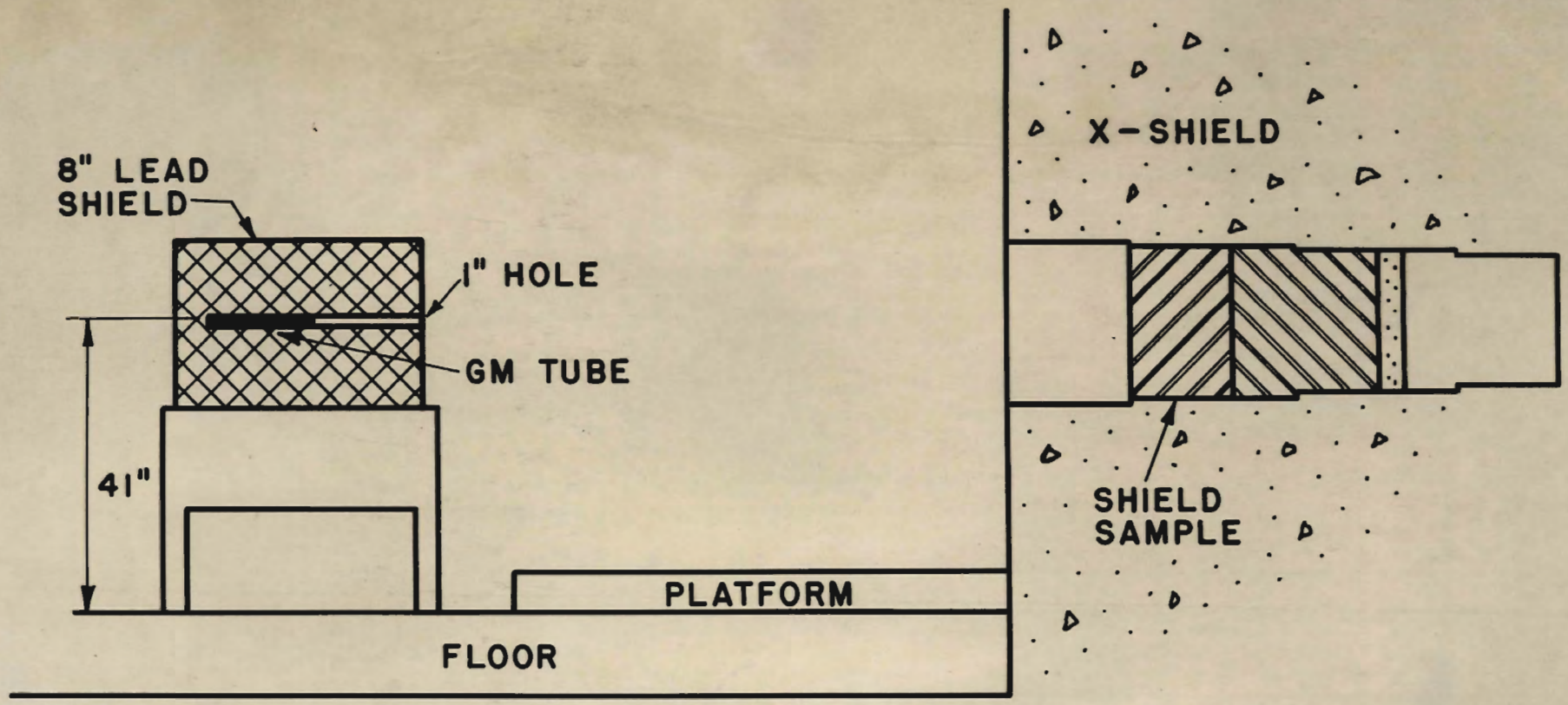

FIG. 17
GAMMA COUNTER ARRANGEMENT

[redacted]

LIST OF TABLES AND FIGURES

Tables

I - V	Neutron data, Hanford shield facsimile
VI - X	Neutron data, MO type shield
1a	Gamma data, Hanford shield facsimile
2a - 6a	Gamma data, MO type shield

Appendix A - Hanford shield facsimile dimensions

Figures

1	Neutron attenuation, Hanford and MO shields
2	" " MO shield with different thermal shields
3	" " MO shield, effect of boron in thermal shield
4	" " MO shield, effect of colemanite behind first 16" of MO
5	γ attenuation, Hanford and MO shields
6	" " MO shield with different thermal shields
7	" " Hanford and MO shields, not corrected for density
8	" " theoretical and experimental data
9	(B-3279) Drawing of shield-testing hole, including arrangement for runs 16, 17 and 21
10	(C-3284) Hanford shield facsimile
11 - 16	Arrangements for runs 22 - 25, 27, 28
17	Gamma counter arrangement